

1 Profiling trace organic chemical biotransformation genes, enzymes and associated bacteria in
2 microbial model communities

3 Lijia Cao¹, Sarahi L. Garcia^{2,3}, Christian Wurzbacher^{1*}

4 ¹ Chair of Urban Water Systems Engineering, Technical University of Munich, Garching, Germany

5 ² Department of Ecology, Environment and Plant Sciences, Science for Life Laboratory, Stockholm
6 University, Stockholm, Sweden

7 ³ Institute for Chemistry and Biology of the Marine environment (ICBM), School of Mathematics
8 and Science, Carl von Ossietzky Universität Oldenburg, Oldenburg, Germany

9 * Correspondence: christian@wurzbacher.cc

10

11 Abstract

12 Microbial biotransformation of trace organic chemicals (TOrcs) is an essential process in
13 wastewater treatment for eliminating environmental pollution. Understanding of TOrc
14 biotransformation mechanisms, especially at their original concentrations, is important to optimize
15 treatment performance, whereas our current knowledge is limited. Here we investigated the
16 biotransformation of seven TOrcs by 24 model communities. The genome-centric analyses
17 unraveled the biotransformation drivers concerning functional genes and enzymes and responsible
18 bacteria. We obtained efficient model communities for complete removal on ibuprofen, caffeine and
19 atenolol, and the transformation efficiencies for sulfamethoxazole, carbamazepine, trimethoprim
20 and gabapentin were 0-45%. Biotransformation performance was not fully reflected by the presence
21 of known biotransformation genes and enzymes. However, functional similar homologs to existing
22 biotransformation genes and enzymes (e.g., long-chain-fatty-acid-CoA ligase encoded by *fadD* and
23 *fadD13* gene, acyl-CoA dehydrogenase encoded by *fadE12* gene) could play critical roles in TOrc
24 metabolism. Finally, we identified previously undescribed degrading strains, e.g., *Rhodococcus*

25 *qingshengii* for caffeine, carbamazepine, sulfamethoxazole and ibuprofen biotransformation, and
26 potential transformation enzymes, e.g., SDR family oxidoreductase targeting sulfamethoxazole and
27 putative hypothetical proteins for caffeine, atenolol and gabapentin biotransformation.

28

29 **Introduction**

30 Trace organic chemicals (TOrcs) (e.g., pharmaceuticals, pesticides, and personal care products)
31 discharged from industries, agriculture, hospitals and households have been frequently detected in
32 natural water sources^{1,2}. The increasing occurrence and accumulation of these ecologically harmful
33 compounds has promoted worldwide research on TOrc removal technologies^{3,4,5}. In general,
34 biological treatment is an effective, economic and energy-saving strategy compared with
35 conventional activated sludge and advanced oxidation processes^{6,7}. Many studies have investigated
36 the microbially mediated degradation of TOrcs and optimized its application in the water and
37 wastewater treatment. For instance, Müller et al.⁸ introduced a novel approach of sequential
38 biofiltration for the advanced treatment of secondary effluent and the pilot-scale experiments
39 confirmed an increased removal of several TOrcs. Edefell et al.⁹ designed a novel process to
40 increase biofilm growth in tertiary moving bed biofilm reactors by providing additional substrate
41 from primary treated wastewater, which significantly improved TOrc removal.

42 Microorganisms play a vital role in the elimination of TOrcs via sorption and biodegradation (full
43 mineralization) or biotransformation (incomplete removal of the parent compound)¹⁰.
44 Biotransformation is considered as the primary removal process for most TOrcs in wastewater
45 treatment plants, which is mainly attributed to oxidative reactions and ammonia oxidizing
46 bacteria^{11,12}. There have been many studies focusing on pure cultures or synthetic microbial
47 consortium that attempted to decipher the metabolic mechanisms including biotransformation
48 byproducts and pathways, key metabolic enzymes, and interspecies interactions^{13,14,15}. Nevertheless,
49 our current knowledge about biotransformation at the level of gene/enzyme-chemical interactions is
50 still limited especially for refractory TOrcs. Addressing this issue is critical for the targeted
51 optimization of biological treatment processes which requires a better understanding of the
52 microbial functionality.

53 In our previous study on the establishment of TOrc-degrading model communities via
54 environmental subset, we obtained eleven taxonomically non-redundant cultivated model

55 communities with different removal abilities on TOrCs¹⁶. Since model communities are well-
56 defined and standardized, they are great tools to identify key driving agents of TOrC
57 biotransformation, i.e., responsible genes and enzymes, and associated microorganisms as well as
58 their functions in the community. However, we observed in our previous study that living in the
59 environment consisting of 27 TOrCs, the biotransformation of individual chemical by model
60 communities was not high-effective and the majority of TOrCs remained unremoved. A hypothesis
61 is that various TOrCs with different physicochemical properties complicate their efficient
62 biotransformation¹⁷. Accordingly, to achieve TOrC-specific promising degraders, here we selected
63 seven TOrCs that are frequently detected in natural water sources, i.e., atenolol, caffeine,
64 carbamazepine, gabapentin, ibuprofen, trimethoprim and sulfamethoxazole. We then transferred 6
65 model communities from our previous study¹⁶ and cultivated *de novo* 18 model communities with
66 the seven chemicals as the substrate either with single chemical or with different mixtures. We
67 obtained the metagenomes of the 24 model communities and comparatively examined (i) the
68 microbial removal performances on the seven TOrCs, (ii) the potential genes and enzymes
69 responsible for the initial metabolic step, and (iii) associated bacteria and the roles they play in the
70 community. The aim of this study is to correlate TOrC biotransformation efficiencies with the
71 presence of currently reported responsible genes and enzymes, and to mine putative novel functions
72 and degraders to expand our knowledge. We hypothesize that TOrC biotransformation efficiencies
73 could be mirrored by the related functional genes and corresponding enzymes. The genome-centric
74 analyses based on these simplified model communities reinforce our understanding of TOrC
75 biotransformation by complementing existing knowledge. Our research could further benefit for
76 designing new approaches for engineering microbes with enhanced biotransformation abilities such
77 as assembly of pathways using enzymes from diverse bacteria to bioremediate TOrC-contaminated
78 environments.

79

80 **Materials and methods**

81 **TOrC selection**

82 Seven TOrCs, atenolol, caffeine, carbamazepine, gabapentin, ibuprofen, trimethoprim and
83 sulfamethoxazole, were selected in this study. These seven TOrCs represent frequently occurring
84 pollutants in municipal wastewater derived with different degree of biodegradability (Table S1).
85 Caffeine and ibuprofen are easy to be biotransformed, and their transformation mechanisms are
86 relatively well documented^{18,19}. Carbamazepine, gabapentin and trimethoprim are rather persistent
87 and poorly biodegradable, and few studies have addressed their biotransformation^{20,21,22}. Atenolol
88 and sulfamethoxazole are reported to be fully or partially degraded by microbial strains^{23,24}. The
89 uses, biotransformation efficiencies, occurrence in aquatic systems, and ecological risks can be
90 found in Table S1.

91 **Model community cultivation**

92 Six model communities were obtained from our previous experiments¹⁶. They were enriched by a
93 mixture of 27 TOrCs and showed biotransformation abilities on the seven investigated compounds.
94 Moreover, we followed the model community establishment workflow that we described before and
95 cultivated another 18 communities. In brief, five samples collected from tap water (Garching,
96 Germany), technical sand treated with tertiary effluent (Garching, Germany), soil (Garching,
97 Germany), surface and deep sediment (47°47'16"N, 11°18'16"E, Osterseen, Germany) on
98 November 2021 were enriched by the seven TOrCs (either individually or jointly, 11 treatments) for
99 six months, resulting in 165 treatment bottles (each TOrC treatment was conducted in triplicate)
100 (Table S2) and 22 blank bottles (11 bottles without cells and 11 bottles with autoclaved cells). The
101 blanks were set as controls to assess the abiotic removal of TOrCs. The enrichment process was
102 divided into six phases with TOrC concentrations set as 50 nmol/L (P1), 250 nmol/L (P2), 500
103 nmol/L (P3), 1000 nmol/L (P4), 2500 nmol/L (P5), 50 nmol/L (P6), respectively. Cell counts were
104 determined by the flow cytometer at the end of each phase to ensure the cell growth following¹⁶.

105 After the enrichment, microbial communities from P6 were then subjected to the dilution-to-
106 extinction step for reducing the species richness. Based on our previous results that enriched
107 microbial communities achieved successful growth above 1×10^6 cells/mL (the ubiquitous density
108 observed in aquatic environment) at the dilution threshold of 10 cells/mL, here we diluted the
109 samples from P6 (pooled triplicates) to 10 cells per well in 96 deep well plates (PP, SARSTEDT,
110 Germany) which contained 1 mL growth medium per well. The growth medium consisted of 5
111 nmol/L TOrCs and mineral salts as described in our previous study¹⁶. Diluted microbes were
112 incubated in the plates in the dark at room temperature for three weeks followed by the
113 measurement of growth. Then, 500 μ L suspension of successful growth wells were transferred to
114 new plates containing 1.5 mL medium per well and were cultivated for two weeks, to get enough
115 volume for the subsequent TOrC removal determination and DNA extraction. Taxonomy refinement
116 was achieved based on the 16S rRNA sequencing (same procedure following Cao et al.¹⁶) and
117 taxonomic assignment by Emu²⁵. The treatment conditions and the preliminary selection of model
118 communities were listed in Table S2.

119 To evaluate the removal rate of each TOrC (not only the feeding TOrC since cultivation) by the 24
120 model communities, 100 μ L suspension of the obtained 24 model communities were added into 1
121 mL medium spiked with 5 nmol/L individual TOrC, and were incubated for three weeks.

122 **Determination of TOrC biotransformation**

123 TOrC reduction was determined using liquid chromatography coupled with tandem mass
124 spectrometry (LC-MS/MS). An ultra-high performance liquid chromatograph (PLATINblue UPLC,
125 Knauer, Germany) was equipped with a Phenomenex Kinetex PFP 100-Å chromatographic column
126 (150×3 mm, 2.6μ m). The UPLC was connected to a Turbo V ion source of a triple quadrupole
127 mass spectrometer (Triple Quad 6500, SCIEX, USA) operated in positive and negative electrospray
128 ionization mode. A binary gradient system was applied, consisting of mobile phase A, Milli-Q water
129 with 0.1% formic acid, and mobile phase B, LC-MS grade acetonitrile (Merck, Germany). Prior to
130 the measurement, 1 mL of samples collected from model community cultivation medium were

131 diluted 2 times to obtain enough volume. 1900 μ L of diluted samples were spiked with 100 μ L of
132 internal standard, and then filtered through 0.22 μ m polyvinylidene difluoride (PVDF) membrane
133 filters into 2 mL amber glass vials for injection. The internal standard method was used for
134 quantification. Isotope-labeled internal standards were available for all analytes. Standard samples
135 at concentrations of 2.5, 5, 10, 25, 50, 100, 250, 500, 1000, 2500, 5000, 10000 ppt were prepared
136 for calibration curves. The data processing was performed on MultiQuant software.

137 **Metagenome sequencing, assembly, binning and taxonomy classification of MAGs**

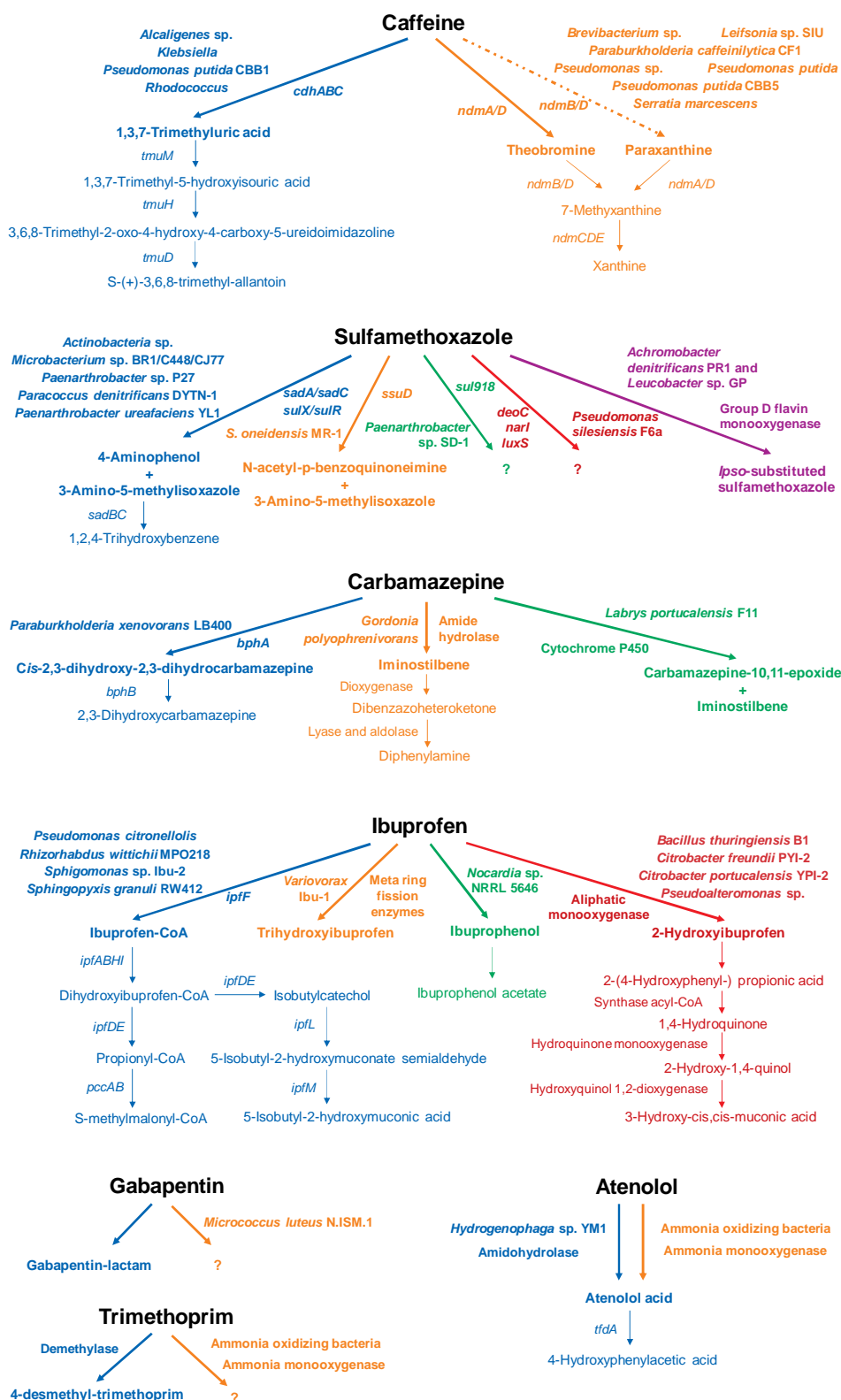
138 DNA was extracted from 24 model communities (600 μ L of each community) using the DNeasy
139 PowerSoil Pro Kit (QIAGEN) according to manufacturers' instruction. Extracted DNA was
140 quantified using dsDNA Broad Range Assay (DeNovix, USA) in a fluorometer (DeNovix, USA).
141 The metagenomic sequencing was performed on PromethION P24 (Oxford Nanopore Technologies)
142 with the R10.4.1 flow cell at LMU Gene Center (Munich, Germany). 100 ng genomic DNA of
143 sample in 12.5 μ L was subjected to prepare a total of 75 μ L library pool using native barcode
144 ligation kit 96 (v14). The average sequencing depth was about 3 Gb per model community.
145 Obtained raw reads were firstly demultiplexed according to their barcodes using Guppy v3.6.0
146 (https://timkahlke.github.io/LongRead_tutorials/BS_G.html). Demultiplexed fast5 reads were
147 duplex-basecalled and converted to FASTQ files using Dorado v0.3.2
148 (<https://github.com/nanoporetech/dorado/>). Barcodes and adapters were also trimmed by Dorado.
149 All sequenced reads from one sample were merged followed by quality control using Filtlong
150 v0.2.1 (<https://github.com/rrwick/Filtlong>) with the parameters "--min_length 1000 --min_mean_q
151 10". Filtered clean reads of each metagenome were assembled and binned by NanoPhase v0.2.3²⁶.
152 Specifically, metaFlye v.2.9-b1768²⁷ was used to assemble trimmed long reads with the option "--
153 nano-hq -i 5 -g 4m". Afterwards, draft metagenome assembled genomes (MAGs) were constructed
154 using MetaBAT2²⁸ and MaxBin2²⁹, and were subjected to the refinement step conducted by
155 MetaWRAP v1.3.2³⁰ to retain the best representative and non-redundant MAGs (completeness > 50%
156 and contamination < 10%). Finally, long reads were mapped to the draft MAGs using minimap2

157 v2.21-r1071³¹ with 90% identity and coverage to produce clusters. Draft MAGs were then polished
158 based on the clusters with one round of Racon v1.4.22 (<https://github.com/isovic/racon>) and one
159 round of medaka v1.4.3 (<https://github.com/nanoporetech/medaka>) to generate high-quality final
160 MAGs. The relative abundance of each MAG was evaluated by SingleM v0.16.0³². The taxonomies
161 of all MAGs derived from 24 model communities were classified by GTDB-Tk v2.3.2³³. The
162 phylogenetic tree of all MAGs based on 120 single-copy marker proteins for bacteria was
163 constructed using the maximum likelihood method via FastTree v2.1.11³⁴ and visualized by iTOL
164 v5³⁵.

165 **Identification of TOrC biotransformation genes, enzymes and pathways**

166 Based on the published literatures, enviPath (a database and prediction system for the microbial
167 biotransformation of organic environmental contaminants)³⁶ and MetaCyc (a curated database of
168 experimentally elucidated metabolic pathways from all domains of life)³⁷, we collected information
169 on the biotransformation pathways, related genes and enzymes, and degrading strains of the seven
170 TOrCs, as shown in Figure 1 and Table S3. The functional annotation of MAGs was conducted by
171 Prokka v1.14.5³⁸ based on the amino acid sequences predicted by Prodigal v2.6.3³⁹. For the genes
172 and enzymes that were not documented in the Prokka annotation databases (e.g. UniProtKB,
173 RefSeq and Pfam), we downloaded their amino acid sequences and identified their homologous
174 proteins using orthoFind with the BLAST e-value as 5e-05, the minimal identity percent from
175 BLAST alignment as 53%, and the minimum length for a domain region as 28⁴⁰. The amino acid
176 sequences were used in a BLAST search to find putative homologous protein. Then, a PSI-BLAST
177 search was performed based on the query sequences and candidate protein sequences to find new
178 and more complete homologous sequences in the Swiss-Prot database. All sequence alignments
179 were produced using ClustalW, and the maximum likelihood trees with 1000 bootstrap were
180 constructed using IQ-TREE v2.2.5⁴¹. The presence of biotransformation genes and enzymes and
181 their homologs were searched against the annotation results of Prokka. Besides the known
182 functional genes and enzymes, we conducted the comparative genomic analysis using OrthoFinder

183 v2.5.5⁴² to identify orthologous groups across 24 model communities and correlate the orthogroups
184 with TOrC removal mining for potential novel biotransformation enzymes. Amino acid sequences
185 of MAGs were merged for each corresponding model community and the concatenated 24 genomes
186 were used as input files in OrthoFinder. DIAMOND and MAFFT were used to the all-versus-all
187 sequence search and multiple sequence alignment, respectively. Gene ontology (GO) functional
188 annotation of the concatenated 24 genomes was performed by PANNZER⁴³. Enrichment of GO
189 terms present in each model community's genes relative to the customized background consisting of
190 all communities' genes was performed using clusterProfiler⁴⁴ in R with the function "enricher" and
191 "compareCluster", and significant enrichment was determined at an adjusted pvalue of 0.05.



192

193 **Figure 1. Overview on currently known biotransformation genes, enzymes, pathways, and**

194 **associated bacteria of caffeine, sulfamethoxazole, carbamazepine, ibuprofen, gabapentin,**

195 **trimethoprim, and atenolol.** Only experimentally validated biotransformation information was
196 included. Colors indicate different metabolic pathways. Bold arrows and text represent the first
197 biotransformation steps and involved genes, enzymes and degraders which were mainly discussed
198 in this study. Question marks represent unknown transformation products. Dash line in caffeine
199 indicates the minor biotransformation pathway.

200

201 **Results and discussion**

202 **TOrC biotransformation efficiencies**

203 The 24 model communities exhibited different removal abilities on the seven TOrCs as shown in
204 Figure 2. In general, most of the communities (19/24) can fully eliminate ibuprofen. While
205 chemicals with aromatic rings are usually resistant to degradation by microorganisms, many studies
206 indicate that ibuprofen is biodegradable despite of its structural characteristics⁴⁵. In a WWTP
207 aeration tank, greater than 95% of ibuprofen was removed with aerobic biodegradation being the
208 dominant mechanism⁴⁶. In a lab-scale cultivated consortium from sewage sludge, 100% of
209 ibuprofen (1 mg/L) was degraded in solution in 6 h and 90% of ibuprofen (10 mg/kg) was degraded
210 in sewage sludge in 16 days⁴⁷. Sulfamethoxazole, carbamazepine and gabapentin can only be
211 partially biotransformed by several model communities with the maximum percentage of 45%, 40%
212 and 42%, respectively. These compounds are often refractive to biodegradation and the reported
213 biological removal efficiencies in water and wastewater treatment are in general below 10%^{20,48,49}.
214 Their chemical structures (e.g., benzene and isoxazole ring in sulfamethoxazole, cyclohexane ring
215 in gabapentin) and potential toxicity to microorganisms⁵⁰ could retard the biotransformation.
216 Caffeine has been reported to be an easily degradable compound with high removal efficiency in
217 WWTP⁵¹, bioreactors⁵², managed aquifer recharge²³ and diverse microbial strains⁵³. Surprisingly, in
218 the present study, only one model community E5 can degrade 100% of caffeine, and other
219 degrading community (A2, A10 and G10) showed merely 22-27% removal, which may point to a
220 preference of ibuprofen over caffeine. Atenolol was reported as a moderately biodegradable

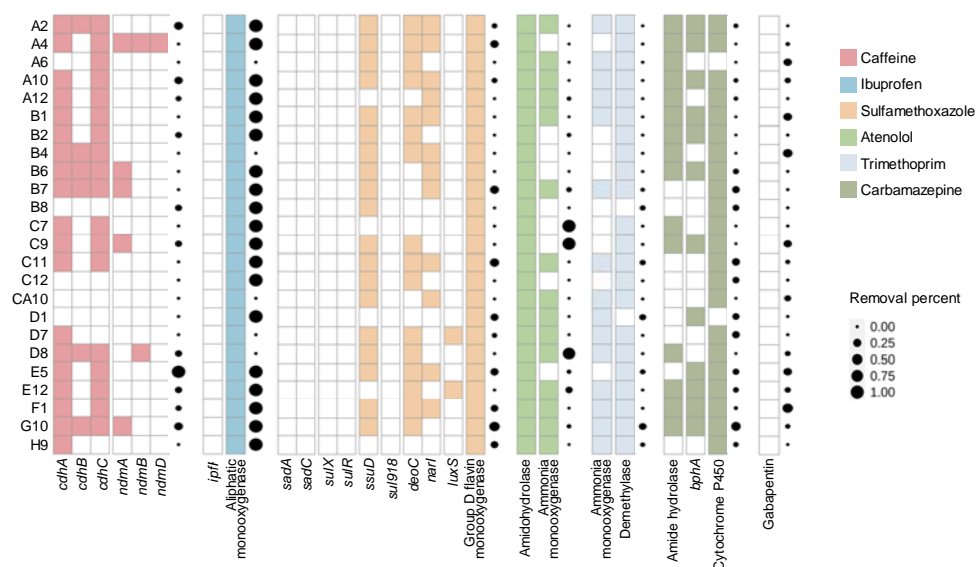
221 compound²³ and trimethoprim is quite recalcitrant^{54,55}. It is consistent in our study that there were
222 three communities (C7, C9 and D8) degrading 85-100% of atenolol and the remaining communities
223 showed none or slight (<27%) removal, while for trimethoprim the average removal efficiency was
224 only 2% among the 24 model communities. Previous studies reported that the kinetics and
225 efficiencies of TOrC biotransformation were impacted by TOrC initial concentration^{56,57,58,59}. For
226 example, pesticide in the low µg/L concentration range often lead to reduced biodegradation^{60,61}.
227 This effect was suggested to be substrate-specific⁶², which might explain the same concentration of
228 the seven TOrCs resulted in different removal limits. Overall, ibuprofen, caffeine and atenolol can
229 be 100% removed by high-efficient degrading model communities with ibuprofen being the most
230 widely removed TOrC. Two model communities removed 23% and 40% of carbamazepine, three
231 communities remove 22-42% of gabapentin, and five communities removed 21-45% of
232 sulfamethoxazole. Trimethoprim was the most persistent chemical that no model community could
233 remove. The community E5 was the best degrader with the ability of biotransforming five TOrCs
234 (i.e., caffeine, ibuprofen, sulfamethoxazole, carbamazepine and gabapentin).

235 **Presence of biotransformation genes and enzymes in model communities**

236 To indicate TOrC removal performance by functional genes and enzymes, we identified the
237 presence/absence of biotransformation genes in the metagenomic annotation results of model
238 communities based on the previous literatures, enviPath and MetaCyc (Figure 2, Table S3). These
239 collected genes and enzymes included first-step biotransformation genes involved in caffeine,
240 ibuprofen, sulfamethoxazole and carbamazepine, and first-step biotransformation enzymes involved
241 in ibuprofen, sulfamethoxazole, atenolol, trimethoprim, carbamazepine and gabapentin. We
242 hypothesized that TOrC biotransformation efficiencies could be mirrored by the related functional
243 genes and enzymes. There were 20 model communities possessing at least one of the *cdhABC* genes
244 responsible for caffeine dehydrogenation (Figure 2). The *ndmA*, *ndmB* and *ndmD* genes involved in
245 caffeine demethylation were present in six model communities (i.e., A4, B6, B7, C9, D8 and G10).
246 Community B8, C12, CA10 and D1 which did not have any caffeine biotransformation genes

247 showed no removal of caffeine. However, not all communities containing related genes could
248 biotransform caffeine, and the best performer E5 only contained *cdhA* and *cdhC* genes which also
249 appeared in other non-degrading model communities (e.g., B1, C7 and C11). It also happened in
250 ibuprofen, sulfamethoxazole, atenolol, trimethoprim and carbamazepine that not all communities
251 having the biotransformation genes and enzymes showed removal on corresponding chemicals, and
252 the same distribution of genes did not indicate similar removal efficiency. For example, aliphatic
253 monooxygenase that metabolize ibuprofen to 2-hydroxyibuprofen was present in all communities,
254 while A6, B4, CA10, D7 and D8 did not reduce any ibuprofen. For gabapentin, although there have
255 been no biotransformation genes or enzymes reported yet, the removal in our study indicated the
256 possibility of previously undescribed functions. The *ipfF*, *sadA*, *sadC*, *sulX*, *sulR* and *sul918* genes
257 were not annotated by Prokka so that they were absent in all communities. In the following section,
258 we identified their homologs to find the potential correlations with TOrC removal.

259 In summary, our hypothesis was partially rejected since the presence of biotransformation genes and
260 enzymes did not fully reflect TOrC removal efficiencies by model communities. The threshold
261 concentration effect (that is, the lowest substrate concentration below which no appreciable growth
262 of specific degrader organisms could be observed that leads to no reduction of substrate)^{63,56}, was
263 suggested to result in the lack of induction of biotransformation gene expression and enzymatic
264 activities^{64,65}. This could also explain the inconsistency between gene presence and not finding
265 corresponding TOrC removal in our study, since the metagenomic analysis shows gene presence but
266 that does not guarantee gene expression. Further metatranscriptomic analysis of functional gene
267 expression patterns is suggested to obtain insights into deciphering the relationships between TOrC
268 presence and the regulation of biotransformation genes and eventually removal performance.

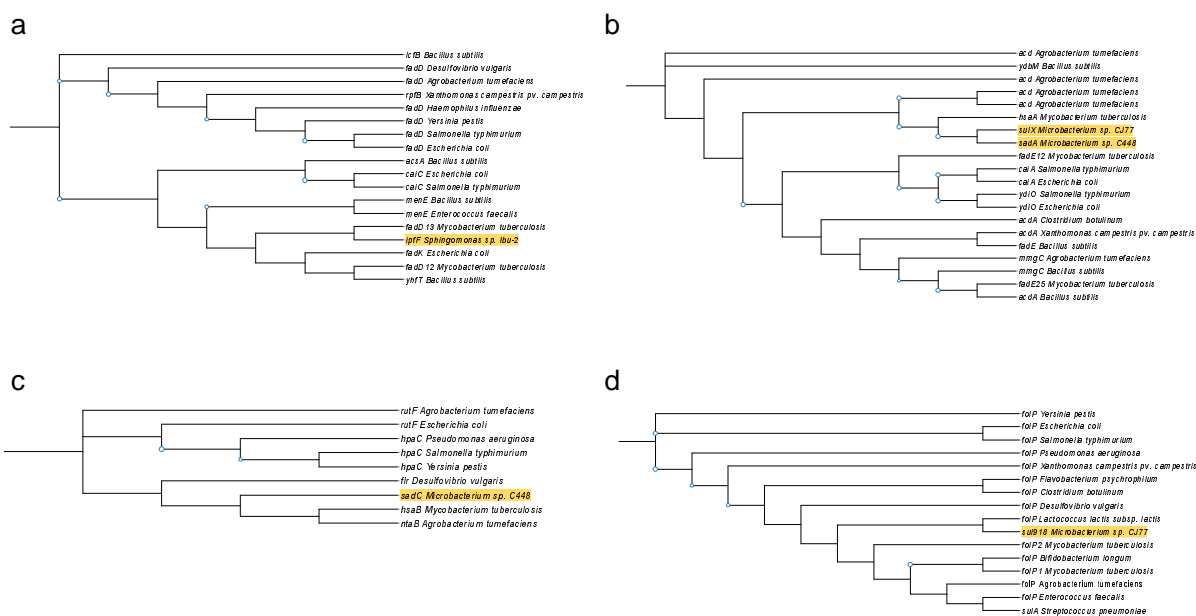


269

270 **Figure 2. TORC biotransformation efficiencies and the presence/absence of first-step**
 271 **biotransformation genes and enzymes in the 24 model communities.** Colors represent presence,
 272 blank represents absence. The dot plot indicates the removal percentage. No biotransformation
 273 genes or enzymes for gabapentin have been reported yet.

274 **Phylogenetic analysis of biotransformation genes and enzymes and their homologs**

275 The *ipfF*, *sadA*, *sadC*, *sulX*, *sulR* and *sul918* genes (responsible for ibuprofen and sulfamethoxazole
 276 biotransformation) were not annotated by Prokka, however, it is likely that these genes may have
 277 diversified in microbial lineages by vertical evolution. Thus, the five genes above were used as
 278 queries to identify potential homologs using orthoFind. Biotransformation genes for caffeine are
 279 well documented so that they were not investigated here. For atenolol, gabapentin and trimethoprim,
 280 their biotransformation genes have not been discovered and are not able to serve as reference
 281 sequences. The number of homologs, functions, domain architecture of the query sequences were
 282 listed in Table S4. Maximum likelihood trees were constructed for the Ipff, SadA, SadC and Sul918
 283 proteins to further investigate the evolutionary links among the various homologs (Figure S1).



284

285 **Figure 3. Phylogenetic trees of (a) ipfF, (b) sadA, (c) sadC, and (d) sul918 genes and their**
 286 **homologs present in model communities.** Homologous proteins were identified based on the
 287 amino acid sequences of these biotransformation genes using OrthoFind. Phylogenetic trees were
 288 constructed using maximum likelihood method by IQ-TREE and modified by iTOL. Bootstrap
 289 support values above 85 are indicated at node.

290 There were 59 homologs to Ipff (ibuprofen CoA ligase) among which CaiC
 291 (crotonobetaine/carnitine-CoA ligase), AscA (acetyl-coenzyme A synthetase), MenE (2-
 292 succinylbenzoate-CoA ligase), YhfT (uncharacterized acyl-CoA ligase), FadK (medium-chain-fatty-
 293 acid-CoA ligase), LcfB (long-chain-fatty-acid-CoA ligase), FadD3 (long-chain-fatty-acid-CoA
 294 ligase), FadD13 (long-chain-fatty-acid-CoA ligase), FadD (long-chain-fatty-acid-CoA ligase) and
 295 RpfB (fatty Acyl-CoA ligase) involved in the ligase activity were present in the 24 model
 296 communities (Figure S1a, Figure 3a). The long-chain-fatty-acid-CoA ligase is known to converting
 297 xenobiotics by targeting the carboxyl or hydroxyl groups as the initial metabolic step. For instance,
 298 Harb et al.⁶⁶ found this enzyme facilitated the biodegradation of two hydroxyl-containing
 299 micropollutants (atenolol and acetaminophen) in an anaerobic MBR system. Pirete et al.⁶⁷ identified
 300 the long-chain-fatty-acid-CoA ligase as the main enzyme involved in diclofenac biotransformation.

301 There were 82 homologous proteins to SadA (sulfonamide monooxygenase) with the function of
302 flavin adenine dinucleotide binding and acyl-CoA dehydrogenase activity which was the same as
303 SulX (Figure S1b, Figure 3b). SulX has been proven to be a homologous protein to SadA⁶⁸. The
304 *hsaA* gene encoding a flavin-dependent monooxygenase located most closely to *sadA* gene among
305 the homologs that can be identified in the model communities. The flavin reductase SadC had 47
306 homologs, HpaC (4-hydroxyphenylacetate 3-monooxygenase reductase component), RutF (FMN
307 reductase), NtaB (FMN reductase), HsaB (flavin-dependent monooxygenase, reductase subunit) and
308 Flr (flavoredoxin) were present in the model communities (Figure S1c, Figure 3c). It was the same
309 to SulR having the identical amino acid sequences with SadC. SadA and SadC were responsible for
310 the initial cleavage of sulfonamides²⁴, and the gene cluster *sulX* and *sulR* containing homologs of
311 SadA and SadC⁶⁸ was also reported to degrade sulfonamides. SadA is highly specific to catalyze the
312 ipso-hydroxylation of sulfamethoxazole releasing 4-aminophenol, while the auxiliary role of SadC
313 in electron transport can easily be replaced by other enzymes with similar function²⁴, indicating the
314 predominant role of SadA in the initial step of sulfamethoxazole biotransformation.

315 The sulfonamide resistant gene *sul918* had most of the homologs characterized as *folP* encoding
316 dihydropteroate synthase (Figure S1d, Figure 3d). The sulfonamide resistance mechanisms are
317 mediated by mutations in *folP* and/or acquisition of *sul* genes. To date the origins of *sul* genes are
318 not clear, but a recent study suggested that the *sul* genes evolved from lateral transfer of
319 chromosomal *folP* genes⁶⁹. Although *sul918* is not the sulfamethoxazole degrading gene, its co-
320 occurrence with *sad* gene cluster was found to favor the efficient degradation of sulfamethoxazole⁷⁰.
321 The possibility of antibiotic resistance genes (e.g., *sulI*, *sul918*) conferring antibiotic
322 biotransformation might indicate the mobilization of biotransformation genes associated with
323 mobile genetic elements between different taxa. Contradictory finding was also reported that a
324 *Paenarthrobacter* strain containing a complete *sad* gene cluster and *sul* genes (*sul918* and *sulI*)
325 displayed limited sulfonamide removal⁷¹. Additional studies are required to decipher the

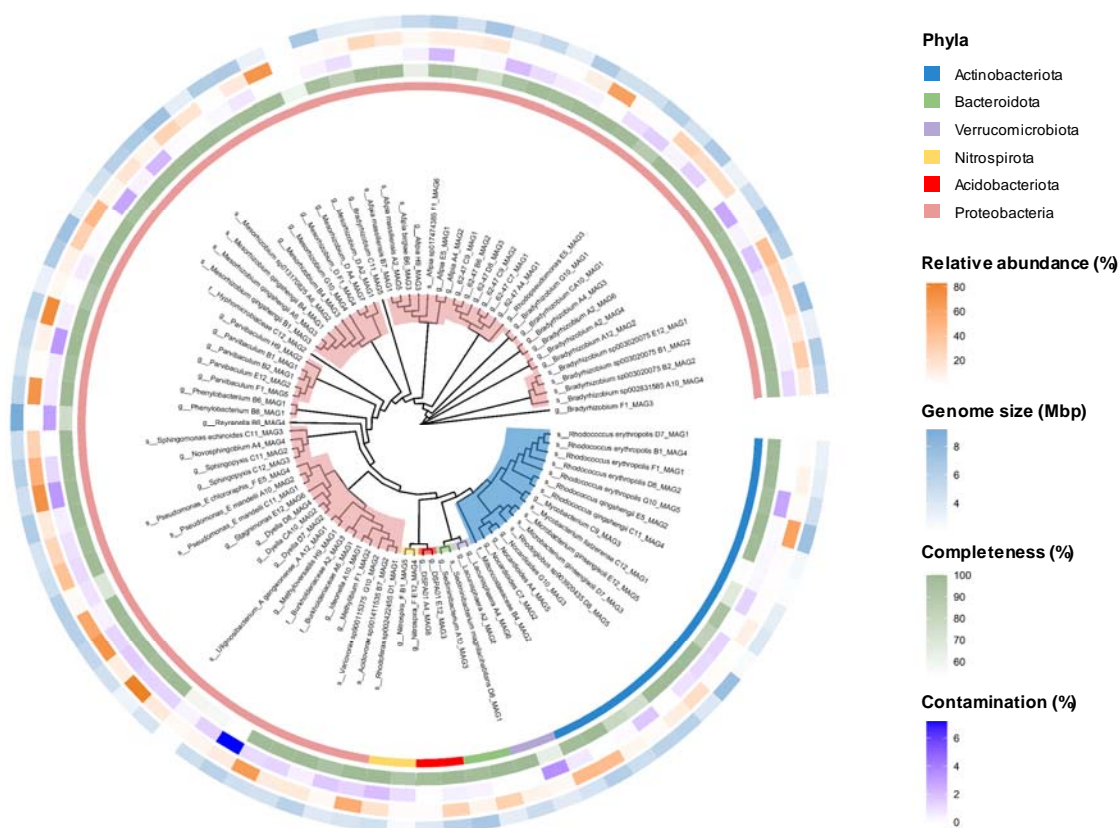
326 relationships between sulfonamide resistance and biotransformation, which is critical for
327 understanding the dissemination of antimicrobial resistance.

328 The known biotransformation genes and enzymes together with their homologs provided us with
329 more comprehensive understanding of the function of members of the same protein family for
330 TORC biotransformation. Phylogenetic analysis of homologs also facilitates the discovery of
331 potential novel biotransformation genes⁷². In many cases, the presence of functional similar
332 homologous proteins acted as surrogates to initiate the metabolic reactions^{68,73,74}. This further points
333 to the possibility of functional gene diversity as an important driver for the transformation of some
334 compounds⁷⁵. However, the homologous proteins often have differences in structure, such as the
335 substrate binding pocket, which could influence TORC binding to the active site of the enzyme and
336 therefore influence the biotransformation efficiency. For example, SadA had a wider pocket than its
337 homolog XiaF, and *Leucobacter* strain GP containing SadA showed better sulfonamide removal
338 than *Microbacterium* sp. BR1 containing XiaF⁷⁶.

339 **Potential biotransformation pathways and associated bacteria carrying related genes and** 340 **enzymes**

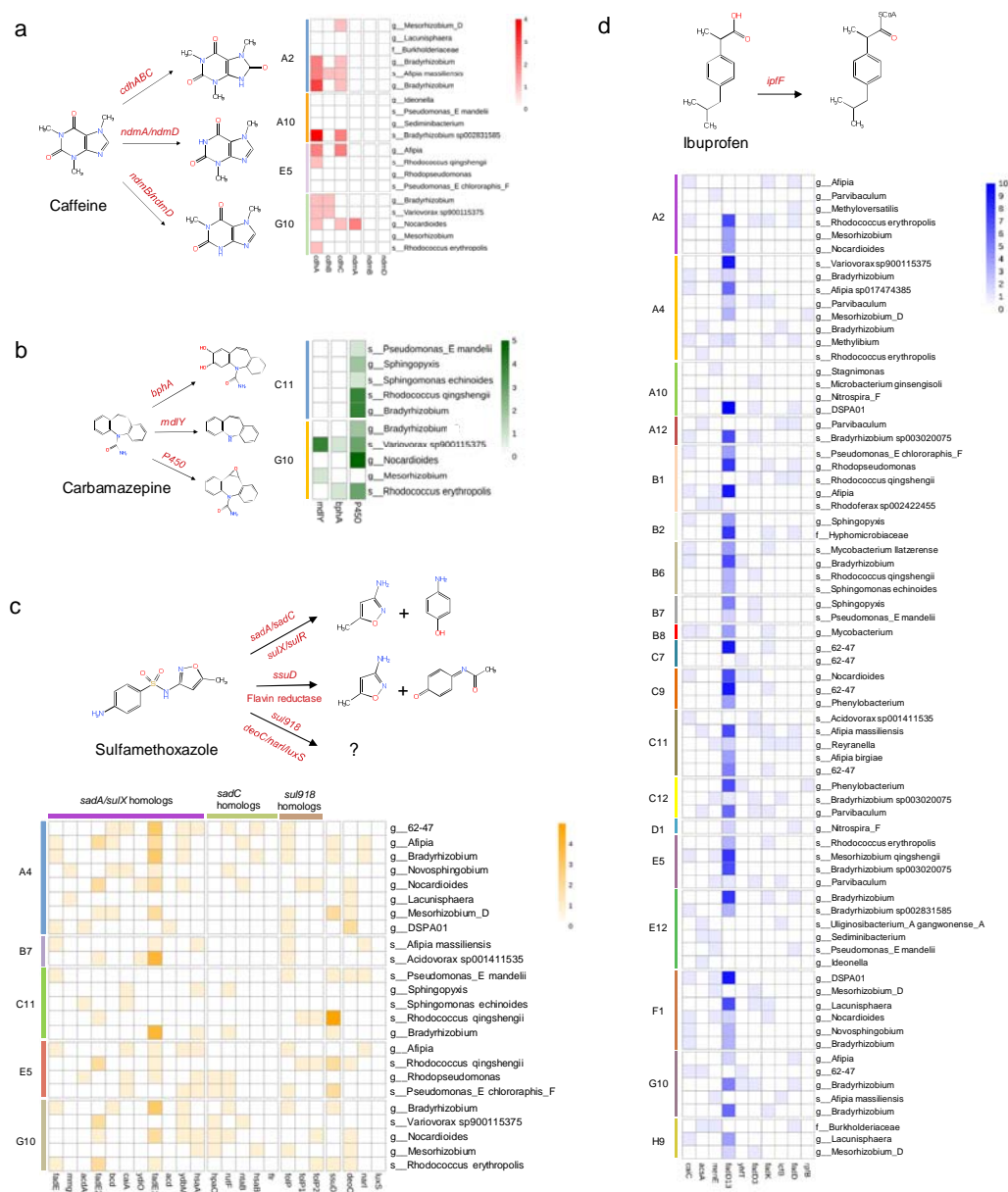
341 To characterize the specific MAGs carrying the biotransformation genes and enzymes, we
342 recovered in total 88 high-quality draft genomes from the 24 model communities' metagenomes
343 (abundance, completeness and contamination are provided in Table S4). Each model community
344 consisted of 1-8 MAGs. According to the Genome Taxonomy Database (GTDB), a total of six phyla
345 were identified with the most abundant phyla being Proteobacteria (n = 64) and Actinobacteriota
346 (n = 16) (Figure 4). Thirty-two of these MAGs were classified to the species level, four MAGs
347 were classified to the family level, and the remaining MAGs were identified to the genus level,
348 indicating novel taxa at different taxonomical levels. Using GTDB nomenclature that newly
349 delineated and uncultured taxa are allocated with alphanumeric placeholder names, we found
350 eighteen MAGs were assigned to genus or species with such placeholder labels (e.g., g_62-47,
351 g_DSPA01, s_Afipia sp017474385, s_Variovorax sp900115375) (Figure 4). Such taxonomic

352 novelty with 75% of MAGs affiliated with new classification is likely driven by niche adaptation to
353 the distinctive cultivation environment where TORCs served as the sole carbon source^{77,78}.
354 Accordingly, the utilization of model communities adapted to TORCs offers us an opportunity to
355 target key microorganisms that are easily submerged in natural microbiome and to uncover their
356 functions that are barely addressed. The frequencies of biotransformation genes and enzymes
357 including their homologs in each MAG of TORC-degrading model communities were determined to
358 identify the main microbial players in the initial biotransformation step (Figure 5).



359

360 **Figure 4. Phylogenetic tree of 88 MAGs derived from the 24 model communities based on 120**
361 **single-copy marker proteins for bacteria constructed using the maximum likelihood method.**
362 The taxonomy was classified by GTDB-Tk.



363

364 **Figure 5. Initial biotransformation pathways, and the presence of related genes and their**
 365 **homologs in the degrading model communities of (a) caffeine, (b) carbamazepine, (c)**
 366 **sulfamethoxazole, and (d) ibuprofen.** Values of the heatmap legend represent the number of genes
 367 identified in each MAG. Gabapentin was excluded since no biotransformation genes or enzymes
 368 have been reported yet. Trimethoprim was excluded since there was no degrading model community.
 369 Atenolol was not shown here but was described in the results section.

370

371 *Caffeine*

372 To date two distinct caffeine biotransformation pathways, *N*-demethylation and C-8 oxidation, has
373 been uncovered in bacteria¹⁸. In the four caffeine-degrading model communities (A2, A10, E5 and
374 G10), the biotransformation genes mainly appeared as the *cdhABC* genes (involved in C-8 oxidation)
375 with only G10 harboring the *ndmA* gene (involved in *N*-demethylation) in one MAG classified to
376 genus *Nocardiodes*. Since *ndmA* is highly dependent on *ndmD*, which is a partner reductase that
377 transfers electrons to power the reaction, the incomplete pathway in G10 suggested the absence of
378 caffeine *N*-demethylation. Hence, caffeine oxidation to 1,3,7-trimethyluric acid was the only
379 pathway in all degrading model communities (Figure 5a). *Bradyrhizobium* carried the most
380 abundant *cdh* genes in community A2, A10 and G10, and *Bradyrhizobium* sp002831585 was the
381 only species carrying *cdhA* and *cdhC* in the community A10, indicating that *Bradyrhizobium* might
382 have the potential of transforming caffeine. In the model community E5, *Afipia* carried *cdhA* and
383 *cdhC* genes and species *Rhodococcus qingshengii* carried only *cdhA* gene. The complete removal of
384 caffeine by E5 suggested that the novel species belonging to *Afipia* and the species *Rhodococcus*
385 *qingshengii* might be the highly efficient caffeine degraders. Upon our survey of caffeine-degrading
386 microorganisms, there have been no reports on caffeine biotransformation by *Bradyrhizobium*,
387 *Afipia* and *Rhodococcus qingshengii* yet, but *Rhodococcus* sp. was found to degrade caffeine via
388 oxidation in a mixture culture with *Klebsiella* sp.⁷⁹. The subsequent transformation steps of 1,3,7-
389 trimethyluric acid involved MAGs lacking *cdh* genes (Figure S2a), indicating the different roles of
390 MAGs in assembling the caffeine oxidation pathway.

391 *Carbamazepine*

392 The first step of carbamazepine biotransformation was accomplished by BphA (biphenyl
393 dioxygenase) metabolizing carbamazepine to cis-10,11-dihydroxy-10,11-dihydrocarbamazepine and
394 cis-2,3-dihydroxy-2,3-dihydrocarbamazepine⁸⁰, amide hydrolase removing the amide group⁸¹, and
395 cytochrome P450 via monooxygenation to carbamazepine-10,11-epoxide²² (Figure 5b).
396 Cytochrome P450 were present in all MAGs except for one MAG affiliated with *Mesorhizobium* of

397 the two carbamazepine-degrading model communities C11 and G10. This is a ubiquitous enzyme
398 system that is important for xenobiotic metabolism in bacteria catalyzing reactions such as aliphatic
399 hydroxylations, epoxidations, and dealkylations⁸². Community C11 only contained cytochrome
400 P450 with its most abundance observed in *Rhodococcus qingshengii* and *Bradyrhizobium*,
401 indicating monooxygenation was the only biotransformation pathway in G10 and *Rhodococcus*
402 *qingshengii* and *Bradyrhizobium* could play a critical role. The *bphA* gene and amide hydrolase
403 encoding gene *mdly* were present only in the community G10 with species *Variovorax*
404 sp900115375 carrying the most abundant *mdly*. *Variovorax* sp900115375 also contained *bphA*.
405 *Mesorthizobium* that lacked the ubiquitous P450 harbored *mdly*, and *Rhodococcus erythropolis*
406 harbored *bphA*. The existence of *mdly* and *bphA* genes in the model community G10 indicated that
407 the metabolism of carbamazepine by G10 could undergo deamidation and hydroxylation pathways
408 in addition to monooxygenation, which might explain the higher removal efficiency in G10 (40%)
409 than C11 (23%). The deamidation could be attributed to *Variovorax* sp900115375 and
410 *Mesorthizobium*, and the hydroxylation could be attributed to *Variovorax* sp900115375 and
411 *Rhodococcus erythropolis*. Biotransformation of organic chemicals requires multifunctionality
412 (multiple metabolic pathways), Stravs et al.⁸³ suggested diverse biotransformation pathways
413 supported by different detected byproducts could enhance the transformation of a broad range of
414 micropollutants in freshwater phytoplankton, that is, functional (pathway) diversity benefits TOrc
415 biotransformation. The unique presence of *bphB* for the next reaction step of carbamazepine
416 hydroxylation in *Rhodococcus erythropolis* in G10 indicated the hydroxylation of carbamazepine
417 was either shared by *Variovorax* sp900115375 and *Rhodococcus erythropolis*, or solely completed
418 by *Rhodococcus erythropolis* (Figure S2b). This suggested the synergistic interaction between
419 members in one model community contributes to TOrc metabolic processes, which were also
420 observed in other recalcitrant chemical degradation studies^{84,85,86}. Although the key degrading
421 bacteria (usually responsible for the first transformation step) are important, the effective
422 performance of a microbial community also depends on the populations targeting intermediates.

423 *Sulfamethoxazole*

424 The known pathways for sulfamethoxazole biotransformation are i) cleavage of the -C-S-N- bond in
425 the sulfonamide molecules leading to 4-aminophenol and 3-amino-5-methylisoxazole by flavin
426 dependent monooxygenase and reductase encoded by *sadA* and *sadC*, respectively²⁴, ii)
427 hydroxylation of aromatic ring by flavin monooxygenase encoded by *ssuD* and flavin reductase⁸⁷.
428 Liu et al.⁸⁸ isolated a highly efficient sulfamethoxazole-degrading strain *Pseudomonas silesiensis*
429 F6a. The *sadA* and *sadC* genes were not identified in its genome, and based on the detected
430 metabolites several key functional genes (e.g., *deoC*, *narI*, *luxS*) participated in C-S cleavage, S-N
431 hydrolysis and isoxazole ring cleavage were proposed. We identified the presence of homologs of
432 SadA and SadC in the MAGs of five sulfamethoxazole-degrading model communities, only B7 did
433 not contain any *sadC* homologs (Figure 5c). In principle, the function of *sadA* requires the
434 assistance of *sadC*, thus the pathway of attacking the -C-S-N- bond was deactivated in B7.
435 Moreover, community B7 did not carry *ssuD* gene, and only *folP* (homolog of *sul918*) and *narI*
436 were present. The sulfonamides resistant gene *sul918* was reported to facilitate the removal of
437 sulfamethoxazole, while itself cannot catalyze sulfamethoxazole. Hence, these observed results
438 pointed out that *narI* could be the key biotransformation gene in B7 and *Afipia massiliensis* might
439 be the potential sulfamethoxazole degrader. FadE12 (acyl-CoA dehydrogenase) was the most
440 abundant SadA homologous protein which appeared mainly in *Bradyrhizobium*, 62-47 and
441 *Acidovorax* sp001411535. *Rhodococcus qingshengii* in community C11 carried the dominant *ssuD*
442 gene which is currently only reported on strain *Shewanella oneidensis* MR-1⁸⁷, indicating its
443 potential importance in sulfamethoxazole hydroxylation. The *sad* gene cluster was found to be
444 conserved in two genera *Paenarthrobacter* and *Microbacterium*⁷¹, it is consistent in our study that
445 no *sadA* or *sadC* was observed in the 88 MAGs with diverse taxonomy. Nevertheless, our study
446 suggested that the functions of *sad* gene cluster could be taken over by their homologs.

447 *Ibuprofen*

448 The *ipfF* gene encoding ibuprofen ligase is responsible for transforming ibuprofen to ibuprofen-
449 CoA⁸⁹. Although *ipfF* was not identified in the degrading model communities, its homologs were
450 characterized (Figure 3a). All 72 MAGs of degrading communities harbored at least one of the Ipff
451 homologous proteins with *fadD13* exhibiting the highest abundance in genera *Bradyrhizobium*, 62-
452 47, *Rhodococcus*, *Sphingopyxis*, *Mycobacterium* and *Rhodopseudomonas* (Figure 5d). The
453 biodiversity of ibuprofen-degrading model communities revealed by species richness varied from
454 one to eight at the MAG level. Stadler et al.⁹⁰ established cultures with a gradient of microbial
455 biodiversity from activated sludge via dilution-to-extinction, and found the loss of biodiversity had
456 a significant correlation with the reduction of biotransformation for atenolol, carbamazepine and
457 venlafaxine. However, ibuprofen biotransformation degree was not affected by the species richness
458 with all degrading communities exhibiting 100% removal. Notably, community B8 and D1
459 consisted of only single MAG affiliated with *Phenylobacterium* and *Rhodoferax* sp002422455,
460 respectively, indicating their unique function in degrading ibuprofen. These two bacteria were
461 reported for the first time in ibuprofen efficient biotransformation. More interestingly, D1 contained
462 only *fadD* and *fadD13* encoding enzyme long-chain-fatty-acid-CoA ligase. This indicated that the
463 long-chain-fatty-acid-CoA ligase is the critical enzyme in ibuprofen biotransformation, and the
464 *fadD* or *fadD13* gene could take the place of *ipfF* gene. The wide distribution of *fadD* and *fadD13*
465 genes also suggested that the CoA ligation to ibuprofen could be driven by diverse bacteria. The
466 existing of other homologs and aliphatic monooxygenase (present in all communities) need further
467 research to confirm whether and how they play a part, which could be supported by transformation
468 products determination, biotransformation experiment on extracted enzyme, and transcripts
469 indicating gene expression.

470 *Atenolol and gabapentin*

471 The first step of atenolol biotransformation pathway was reported to be the acetylation of the amino
472 group catalyzed by amidohydrolase, and the related bacterium was *Hydrogenophaga*⁹¹. In the
473 present study, amidohydrolase was identified in all 88 MAGs, while only three communities can

474 degrade atenolol. Ammonia monooxygenase was also found to convert atenolol to atenolol acid by
475 ammonia oxidizing bacteria⁹², and it only appeared in *Dyella* in D8 community and was absent in
476 the other two atenolol-degrading community C7 and C9. The roles of amidohydrolase and ammonia
477 monooxygenase still need further investigation regarding their expression or activity. Gabapentin
478 was reported to be transformed to gabapentin-lactam via intramolecular amidation in the biological
479 process⁹³ while the related enzymes have not been addressed yet. Community B4 and F1 removed
480 32% and 42% of gabapentin, respectively. Our results indicated that there could also be novel
481 functions and pathways for atenolol and gabapentin biotransformation that are unmined.

482 In summary, in this section we discussed the known biotransformation genes, enzymes and
483 pathways for caffeine, carbamazepine, ibuprofen, sulfamethoxazole, atenolol and gabapentin.
484 Trimethoprim was excluded since no model community showed removal on it. We then related the
485 distribution of these biotransformation agents to the removal efficiencies of model communities,
486 and inferred potential associated degrading bacteria and functional alternatives (homologs). We
487 found that caffeine oxidation to 1,3,7-trimethyluric acid was the dominant pathway, with
488 *Bradyrhizobium*, *Afipia* and *Rhodococcus qingshengii* acting as potential degraders that are reported
489 for the first time. Carbamazepine biotransformation could be enhanced by the involvement of
490 cytochrome P450, *mdlY* and *bphA* providing multiple pathways, *Rhodococcus qingshengii*,
491 *Rhodococcus erythropolis*, *Bradyrhizobium*, *Variovorax sp900115375* and *Mesorhizobium* might
492 be the associated bacteria. The long-chain-fatty-acid-CoA ligase was found to be the critical enzyme
493 in ibuprofen biotransformation, and the *fadD* and *fadD13* gene could function as *ipfF* gene.
494 Efficient ibuprofen biotransformation could be driven by diverse microorganisms. The *sad* gene
495 cluster responsible for sulfamethoxazole biotransformation was not identified in the degrading
496 model communities, but *sadA*'s homolog *fadE12* was abundant in *Bradyrhizobium*, 62-47 and
497 *Acidovorax sp001411535*. Notably, *Rhodococcus qingshengii* has been reported to be able to
498 degrade carbendazim⁹⁴, phenanthrene⁹⁵, triphenylmethane dyes⁹⁶, phenol⁹⁷, naphthalene⁹⁸, and
499 crude oil⁹⁹. Our results showed that *Rhodococcus qingshengii* also carried caffeine, carbamazepine,

500 sulfamethoxazole and ibuprofen biotransformation genes and enzymes, and the removal
501 performance indicated its potential ability in various TOrC metabolism. For atenolol, gabapentin
502 and trimethoprim, since their current biotransformation knowledge is scarce, more experiments on
503 degrading model communities (e.g., pure culture isolation, transformation products detection,
504 enzyme-based degradation, gene expression) are required to confirm the function of reported
505 enzymes (e.g., amidase, amidohydrolase) and to explore novel pathways.

506 **Comparative genomic analyses indicated potential novel functions**

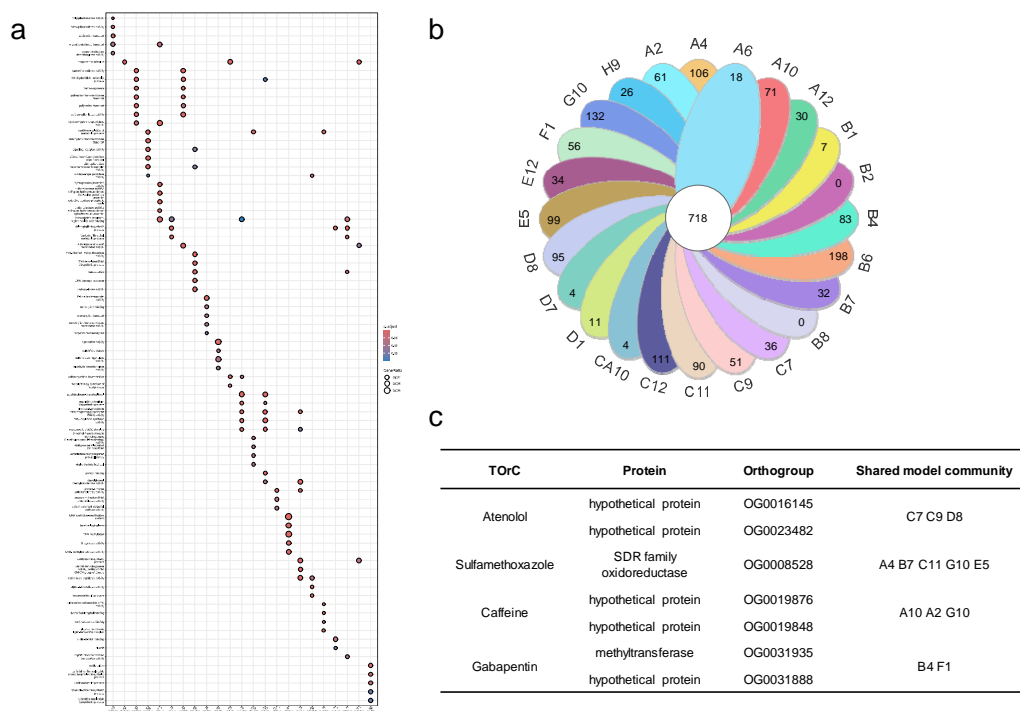
507 The known pathways and biotransformation agents discussed in the above sections provided us with
508 an overview of their existence in the 24 model communities. However, the unknown mechanisms
509 still need further research to deepen our understanding of various TOrC biotransformation by
510 diverse species. Here, we conducted comparative genomic analyses via GO enrichment and related
511 gene family prediction, aiming to discover potential novel functions shared by model communities
512 with similar TOrC removal performance. The GO enrichment analysis compared the significantly
513 enriched functions among the 24 model communities (Figure 6a). In general, most model
514 communities possessed their unique functions, while B4 and A6, C9 and C12 shared similar GO
515 modules. To be specific, community A6 consisted of a dominant strain belonging to
516 Burkholderiaceae (69.8%) and two *Mesorhizobium* strains (13.8% and 0.7%), B4 was dominated by
517 *Mesorhizobium* (75.9% and 8.3%) and 4.3% was from Miltoncostaeales. Although they were
518 dominated by different bacteria, their biological functions were both enriched in sarcosine oxidase
519 activity, tetrahydrofolate metabolic process, methanogenesis, polyamine transmembrane transport
520 and carbon-sulfur lyase activity, and these two communities showed similar TOrC removal
521 performance that can only biotransform gabapentin (A6: 21% and B4: 32%). The community C9
522 which could biotransform 100% ibuprofen and atenolol was composed by three strains belonging to
523 genera 62-47 (26.8% and 40.4%) and *Mycobacterium* (3.4%), and community C12 degrading only
524 ibuprofen consisted of three strains from species *Mycobacterium llatzerense* (13.2%), genus
525 *Sphingopyxis* (54.7%) and family Hyphomicroblaceae (3.8%). Peptidoglycan-based cell wall,

526 regulation of cellular biosynthetic process, glucose-6-phosphate dehydrogenase (coenzyme F420)
527 activity, fatty-acyl-CoA synthase activity, and response to abiotic stimulus were the functions shared
528 by C9 and C12. The community E5 was the best degrader that biotransformed the most TORCs (i.e.,
529 caffeine, ibuprofen, sulfamethoxazole, carbamazepine and gabapentin), showing the unique
530 enrichment in glutamate synthase (NADPH) activity, bacteriochlorophyll binding, toxic substance
531 binding and plasma membrane light-harvesting complex. The GO enriched analysis in model
532 communities could indicate the association between these enriched functions and specific TORC
533 biotransformation. A supportive example is that the fatty-acyl-CoA synthase activity enriched in
534 ibuprofen-degrading communities (C9 and C12) is related to transformation of ibuprofen to
535 ibuprofen-CoA.

536 Furthermore, in order to find uncharacterized putative biotransformation functions, we used
537 OrthoFinder to access orthologous clusters of the 24 model communities. As a result, OrthoFinder
538 assigned 414772 genes (94.5 % of total) to 36064 orthogroups, 718 of which were found in all 24
539 concatenated genomes, and 1355 of which were community-specific orthogroups that were only
540 present in one genome (Figure 6b). The sulfamethoxazole degrader A4, B7, C11, G10 and E5
541 shared only one orthogroup with the function of SDR (short-chain dehydrogenases/reductases)
542 family oxidoreductase. SDR enzymes play important roles in lipid, amino acid, carbohydrate,
543 cofactor, hormone and xenobiotic metabolism¹⁰⁰. Interestingly, some studies have shown that the
544 SDR family enzymes are upregulated in microbes when they are challenged with organic
545 pollutants^{101,102,103,104}. These findings support our preliminary data that the SDR family
546 oxidoreductase could be involved in sulfamethoxazole biotransformation. There were two
547 hypothetical protein orthogroups identified in caffeine degrading community A10, A2 and G10 and
548 no shared orthogroups were found when we included E5. This might suggest that the difference of
549 caffeine removal efficiency between E5 and the other three communities (A10, A2, G10) might be
550 attributed to their functional divergence. The atenolol degrader C7, C9 and D8 shared two
551 orthogroups identified as hypothetical protein that have not been annotated yet. For gabapentin

552 degrading community B4 and F1, they shared one hypothetical protein orthogroup and another
 553 characterized as methyltransferase. Considering the chemical structure of gabapentin, it is unlikely
 554 the methyltransferase would act on the functional groups or ring in the first step of transformation,
 555 but it might be involved in subsequent reactions if gabapentin is attacked by other enzymes
 556 resulting in structural modification. Nevertheless, our inference needs further experiments to
 557 validate. Moreover, the functional annotation of identified promising hypothetical proteins
 558 (sequences were provided in Table S6) also requires further investigation in our future research.

559 Hence, by using the comparative analyses we proposed enriched functions and putative
 560 biotransformation enzymes based on the TOrC-degrading and non-degrading model communities
 561 (Table S6). However, since the model communities were shaped by diverse species and showed
 562 different degrees of TOrC removal, the prediction of gene families related to each TOrC
 563 biotransformation is not that straightforward. In the future work, it could be more reliable to apply
 564 transcriptomic analysis to analyze the upregulated enzymes or differential expressed genes.



566 **Figure 6. Comparative genomic analyses unraveling potential uncharacterized**
567 **biotransformation functions.** (a) Gene ontology (GO) functional annotation and enrichment of the
568 24 model communities. The x axis is model communities with the number of genes annotated with
569 GO terms. The y axis is the description of GO terms. The color and size of the dots represent the
570 significance of GO terms, and the gene ratio (the percentage of differentially expressed genes in a
571 given GO term), respectively. (b) Venn diagram showing the shared and unique orthogroups among
572 the 24 model communities identified using OrthoFinder. (c) Shared orthogroups of TOrC specific
573 degrading model communities indicating putative novel biotransformation enzymes. The sequences
574 of each orthogroup were provided in Table S5.

575

576 **Conclusions**

577 In this study, we obtained 24 bacterial model communities with one to eight taxa by adapting them
578 to seven TOrCs (i.e., atenolol, caffeine, carbamazepine, gabapentin, ibuprofen, sulfamethoxazole,
579 trimethoprim) prior to dilution-to-extinction. In addition, we profiled the biotransformation genes,
580 enzymes and associated bacteria of each TOrC by metagenome-centric analyses integrated with
581 currently known biotransformation knowledge. Our research was conducted on adaptation-dilution-
582 cultivation model communities in response to real-world TOrC concentrations, filling out the
583 knowledge for both well-understood chemicals (e.g., caffeine) and less well-understood TOrCs (e.g.,
584 carbamazepine, gabapentin). Our main findings are:

585 i) The 24 model communities exhibited different TOrC removal abilities and we achieved several
586 efficient degraders for ibuprofen (100% removal), caffeine (100% removal) and atenolol (85-100%
587 removal). The transformation efficiencies for other TOrCs ranged from 0% to 45% with almost no
588 removal on trimethoprim. The community E5 was the best degrader with the ability of
589 biotransforming multiple organic chemicals of diverse structures: caffeine, ibuprofen,
590 sulfamethoxazole, carbamazepine and gabapentin.

591 ii) The presence of initial biotransformation genes and enzymes did not fully support the
592 corresponding TORC removal, and further expression level validation is needed. Functional similar
593 homologs to existing biotransformation genes and enzymes could play critical roles in TORC
594 metabolism. Long-chain-fatty-acid-CoA ligase encoded by *fadD* and *fadD13* gene could be
595 responsible for CoA ligation to ibuprofen. Acyl-CoA dehydrogenase encoded by *fadE12* gene could
596 function as SadA to transform sulfamethoxazole by attacking the -C-S-N- bond.

597 iii) Novel TORC-degraders were reported for the first time. *Bradyrhizobium*, *Afipia* and
598 *Rhodococcus qingshengii* were potential caffeine-degrading bacteria. *Rhodococcus qingshengii*,
599 *Rhodococcus erythropolis*, *Bradyrhizobium*, *Variovorax sp900115375* and *Mesorhizobium* might
600 be carbamazepine-degrading associated bacteria. *Bradyrhizobium*, 62-47 and *Acidovorax*
601 *sp001411535* could be responsible for sulfamethoxazole biotransformation. *Rhodococcus*
602 *qingshengii* carrying caffeine, carbamazepine, sulfamethoxazole and ibuprofen biotransformation
603 genes and enzymes could be a promising species for multiple TORC removal.

604 iii) SDR family oxidoreductase could be involved in sulfamethoxazole biotransformation. Novel
605 putative hypothetical proteins were identified in caffeine, atenolol and gabapentin degrading model
606 communities, but their functions as well as resulting pathways require further analysis.

607

608 **Data availability**

609 Raw metagenome sequencing data and assembled MAGs have been deposited at INSDC (with
610 ENA: <https://www.ebi.ac.uk/ena>) under the project accession number PRJEB74141.

611

612 **Acknowledgments**

613 This study was funded by the German Research Foundation (DFG, WU 890/2-1) and China
614 Scholarship Council (LC). We are grateful to Leibniz-Rechenzentrum for providing computational

615 resources. Ignacio Fernando Sottorff Neculhueque and Javad Ahmadi are thanked for assisting the
616 LC-MS/MS measurement. Laboratory for Functional Genome Analysis (LAFUGA) of the Ludwig-
617 Maximilian-University Munich is thanked for performing the high-throughput sequencing.

618

619 **Author contributions**

620 LC and CW designed this research; LC performed the experiments, analyzed the data and drafted
621 the manuscript; CW and SLG guided the data analysis and revised the manuscript. All authors read
622 and approved the final manuscript.

623

624 **Competing interests**

625 All authors declare no competing interests.

626 **References**

- 627 1. Schulze, S. *et al.* Occurrence of emerging persistent and mobile organic contaminants in
628 European water samples. *Water Res.* **153**, 80–90 (2019).
- 629 2. Mladenov, N. *et al.* Persistence and removal of trace organic compounds in centralized and
630 decentralized wastewater treatment systems. *Chemosphere* **286**, 131621 (2022).
- 631 3. Miklos, D. B., Wang, W.-L., Linden, K. G., Drewes, J. E. & Hübner, U. Comparison of UV-
632 AOPs (UV/H₂O₂, UV/PDS and UV/Chlorine) for TO_{RC} removal from municipal wastewater
633 effluent and optical surrogate model evaluation. *Chem. Eng. J.* **362**, 537–547 (2019).
- 634 4. Tufail, A., Price, W. E., Mohseni, M., Pramanik, B. K. & Hai, F. I. A critical review of
635 advanced oxidation processes for emerging trace organic contaminant degradation:
636 Mechanisms, factors, degradation products, and effluent toxicity. *J. Water Process Eng.* **40**,
637 101778 (2021).
- 638 5. Li, Y. *et al.* Enhanced removal of trace pesticides and alleviation of membrane fouling using
639 hydrophobic-modified inorganic-organic hybrid flocculants in the flocculation-sedimentation-
640 ultrafiltration process for surface water treatment. *Water Res.* **229**, 119447 (2023).
- 641 6. Zearley, T. L. & Summers, R. S. Removal of Trace Organic Micropollutants by Drinking
642 Water Biological Filters. *Environ. Sci. Technol.* **46**, 9412–9419 (2012).
- 643 7. Kanaujiya, D. K., Paul, T., Sinharoy, A. & Pakshirajan, K. Biological Treatment Processes for
644 the Removal of Organic Micropollutants from Wastewater: a Review. *Curr. Pollut. Rep.* **5**,
645 112–128 (2019).
- 646 8. Müller, J., Drewes, J. E. & Hübner, U. Sequential biofiltration – A novel approach for
647 enhanced biological removal of trace organic chemicals from wastewater treatment plant
648 effluent. *Water Res.* **127**, 127–138 (2017).
- 649 9. Edefell, E. *et al.* Promoting the degradation of organic micropollutants in tertiary moving bed
650 biofilm reactors by controlling growth and redox conditions. *J. Hazard. Mater.* **414**, 125535
651 (2021).

- 652 10. Rios-Miguel, A. B. *et al.* Predicting and improving the microbial removal of organic
653 micropollutants during wastewater treatment: A review. *Chemosphere* **333**, 138908 (2023).
- 654 11. Xu, Y., Yuan, Z. & Ni, B.-J. Biotransformation of pharmaceuticals by ammonia oxidizing
655 bacteria in wastewater treatment processes. *Sci. Total Environ.* **566–567**, 796–805 (2016).
- 656 12. Ngo, H. H. *et al.* Chapter 8 - Biotransformation of organic micro-pollutants in biological
657 wastewater. in *Current Developments in Biotechnology and Bioengineering* (eds. Varjani, S.,
658 Pandey, A., Tyagi, R. D., Ngo, H. H. & Larroche, C.) 185–204 (Elsevier, 2020).
659 doi:10.1016/B978-0-12-819594-9.00008-5.
- 660 13. Deng, Y., Wang, Y., Mao, Y. & Zhang, T. Partnership of *Arthrobacter* and *Pimelobacter* in
661 Aerobic Degradation of Sulfadiazine Revealed by Metagenomics Analysis and Isolation.
662 *Environ. Sci. Technol.* **52**, 2963–2972 (2018).
- 663 14. Ghatge, S. *et al.* A novel pathway for initial biotransformation of dinitroaniline herbicide
664 butralin from a newly isolated bacterium *Sphingopyxis* sp. strain HMH. *J. Hazard. Mater.* **402**,
665 123510 (2021).
- 666 15. Zhang, J. *et al.* Deciphering chloramphenicol biotransformation mechanisms and microbial
667 interactions via integrated multi-omics and cultivation-dependent approaches. *Microbiome* **10**,
668 180 (2022).
- 669 16. Cao, L., Garcia, S. L. & Wurzbacher, C. Establishment of microbial model communities
670 capable of removing trace organic chemicals for biotransformation mechanisms research.
671 *Microb. Cell Factories* **22**, 245 (2023).
- 672 17. Hou, L., Kumar, D., Yoo, C. G., Gitsov, I. & Majumder, E. L.-W. Conversion and removal
673 strategies for microplastics in wastewater treatment plants and landfills. *Chem. Eng. J.* **406**,
674 126715 (2021).
- 675 18. Summers, R. M., Mohanty, S. K., Gopishetty, S. & Subramanian, M. Genetic characterization
676 of caffeine degradation by bacteria and its potential applications. *Microb. Biotechnol.* **8**, 369–
677 378 (2015).

- 678 19. Žur, J. *et al.* Organic micropollutants paracetamol and ibuprofen—toxicity, biodegradation,
679 and genetic background of their utilization by bacteria. *Environ. Sci. Pollut. Res.* **25**, 21498–
680 21524 (2018).
- 681 20. Herrmann, M., Menz, J., Olsson, O. & Kümmerer, K. Identification of phototransformation
682 products of the antiepileptic drug gabapentin: Biodegradability and initial assessment of
683 toxicity. *Water Res.* **85**, 11–21 (2015).
- 684 21. Jewell, K. S. *et al.* New insights into the transformation of trimethoprim during biological
685 wastewater treatment. *Water Res.* **88**, 550–557 (2016).
- 686 22. Bessa, V. S., Moreira, I. S., Murgolo, S., Mascolo, G. & Castro, P. M. L. Carbamazepine is
687 degraded by the bacterial strain *Labrys portucalensis* F11. *Sci. Total Environ.* **690**, 739–747
688 (2019).
- 689 23. Alidina, M., Li, D., Ouf, M. & Drewes, J. E. Role of primary substrate composition and
690 concentration on attenuation of trace organic chemicals in managed aquifer recharge systems.
691 *J. Environ. Manage.* **144**, 58–66 (2014).
- 692 24. Ricken, B. *et al.* FMNH2-dependent monooxygenases initiate catabolism of sulfonamides in
693 *Microbacterium* sp. strain BR1 subsisting on sulfonamide antibiotics. *Sci. Rep.* **7**, 15783
694 (2017).
- 695 25. Curry, K. D. *et al.* Emu: species-level microbial community profiling of full-length 16S rRNA
696 Oxford Nanopore sequencing data. *Nat. Methods* **19**, 845–853 (2022).
- 697 26. Liu, L., Yang, Y., Deng, Y. & Zhang, T. Nanopore long-read-only metagenomics enables
698 complete and high-quality genome reconstruction from mock and complex metagenomes.
699 *Microbiome* **10**, 1–7 (2022).
- 700 27. Kolmogorov, M. *et al.* metaFlye: scalable long-read metagenome assembly using repeat
701 graphs. *Nat. Methods* **17**, 1103–1110 (2020).
- 702 28. Kang, D. D. *et al.* MetaBAT 2: an adaptive binning algorithm for robust and efficient genome
703 reconstruction from metagenome assemblies. *PeerJ* **7**, e7359 (2019).

- 704 29. Wu, Y.-W., Simmons, B. A. & Singer, S. W. MaxBin 2.0: an automated binning algorithm to
705 recover genomes from multiple metagenomic datasets. *Bioinformatics* **32**, 605–607 (2016).
- 706 30. Uritskiy, G. V., DiRuggiero, J. & Taylor, J. MetaWRAP—a flexible pipeline for genome-
707 resolved metagenomic data analysis. *Microbiome* **6**, 158 (2018).
- 708 31. Li, H. Minimap2: pairwise alignment for nucleotide sequences. *Bioinformatics* **34**, 3094–3100
709 (2018).
- 710 32. Woodcroft, B. J. *et al.* SingleM and Sandpiper: Robust microbial taxonomic profiles from
711 metagenomic data. 2024.01.30.578060 Preprint at <https://doi.org/10.1101/2024.01.30.578060>
712 (2024).
- 713 33. Chaumeil, P.-A., Mussig, A. J., Hugenholtz, P. & Parks, D. H. GTDB-Tk v2: memory friendly
714 classification with the genome taxonomy database. *Bioinformatics* **38**, 5315–5316 (2022).
- 715 34. Price, M. N., Dehal, P. S. & Arkin, A. P. FastTree 2 – Approximately Maximum-Likelihood
716 Trees for Large Alignments. *PLOS ONE* **5**, e9490 (2010).
- 717 35. Letunic, I. & Bork, P. Interactive Tree Of Life (iTOL): an online tool for phylogenetic tree
718 display and annotation. *Bioinformatics* **23**, 127–128 (2007).
- 719 36. Wicker, J. *et al.* enviPath – The environmental contaminant biotransformation pathway
720 resource. *Nucleic Acids Res.* **44**, D502–D508 (2016).
- 721 37. Caspi, R. *et al.* The MetaCyc database of metabolic pathways and enzymes - a 2019 update.
722 *Nucleic Acids Res.* **48**, D445–D453 (2020).
- 723 38. Seemann, T. Prokka: rapid prokaryotic genome annotation. *Bioinformatics* **30**, 2068–2069
724 (2014).
- 725 39. Hyatt, D. *et al.* Prodigal: prokaryotic gene recognition and translation initiation site
726 identification. *BMC Bioinformatics* **11**, 119 (2010).
- 727 40. Mier, P., Andrade-Navarro, M. A. & Pérez-Pulido, A. J. orthoFind Facilitates the Discovery of
728 Homologous and Orthologous Proteins. *PLOS ONE* **10**, e0143906 (2015).

- 729 41. Minh, B. Q. *et al.* IQ-TREE 2: New Models and Efficient Methods for Phylogenetic Inference
730 in the Genomic Era. *Mol. Biol. Evol.* **37**, 1530–1534 (2020).
- 731 42. Emms, D. M. & Kelly, S. OrthoFinder: solving fundamental biases in whole genome
732 comparisons dramatically improves orthogroup inference accuracy. *Genome Biol.* **16**, 157
733 (2015).
- 734 43. Törönen, P. & Holm, L. PANNZER—A practical tool for protein function prediction. *Protein*
735 *Sci.* **31**, 118–128 (2022).
- 736 44. Yu, G., Wang, L.-G., Han, Y. & He, Q.-Y. clusterProfiler: an R Package for Comparing
737 Biological Themes Among Gene Clusters. *OMICS J. Integr. Biol.* **16**, 284–287 (2012).
- 738 45. Jan-Roblero, J. & Cruz-Maya, J. A. Ibuprofen: Toxicology and Biodegradation of an Emerging
739 Contaminant. *Molecules* **28**, 2097 (2023).
- 740 46. Smook, T. M., Zho, H. & Zytner, R. G. Removal of ibuprofen from wastewater: comparing
741 biodegradation in conventional, membrane bioreactor, and biological nutrient removal
742 treatment systems. *Water Sci. Technol.* **57**, 1–8 (2008).
- 743 47. Aguilar-Romero, I., Madrid, F., Villaverde, J. & Morillo, E. Ibuprofen-enhanced
744 biodegradation in solution and sewage sludge by a mineralizing microbial consortium. Shift in
745 associated bacterial communities. *J. Hazard. Mater.* **464**, 132970 (2024).
- 746 48. Kosjek, T., Andersen, H. R., Kompare, B., Ledin, A. & Heath, E. Fate of Carbamazepine
747 during Water Treatment. *Environ. Sci. Technol.* **43**, 6256–6261 (2009).
- 748 49. Yan, R., Wang, Y., Li, J., Wang, X. & Wang, Y. Determination of the lower limits of antibiotic
749 biodegradation and the fate of antibiotic resistant genes in activated sludge: Both nitrifying
750 bacteria and heterotrophic bacteria matter. *J. Hazard. Mater.* **425**, 127764 (2022).
- 751 50. Iranzo, M., Gamón, M., Boluda, R. & Mormeneo, S. Analysis of pharmaceutical
752 biodegradation of WWTP sludge using composting and identification of certain
753 microorganisms involved in the process. *Sci. Total Environ.* **640–641**, 840–848 (2018).

- 754 51. Baalbaki, Z., Torfs, E., Yargeau, V. & Vanrolleghem, P. A. Predicting the fate of
755 micropollutants during wastewater treatment: Calibration and sensitivity analysis. *Sci. Total*
756 *Environ.* **601–602**, 874–885 (2017).
- 757 52. Katam, K., Shimizu, T., Soda, S. & Bhattacharyya, D. Performance evaluation of two trickling
758 filters removing LAS and caffeine from wastewater: Light reactor (algal-bacterial consortium)
759 vs dark reactor (bacterial consortium). *Sci. Total Environ.* **707**, 135987 (2020).
- 760 53. Korekar, G., Kumar, A. & Ugale, C. Occurrence, fate, persistence and remediation of caffeine:
761 a review. *Environ. Sci. Pollut. Res.* **27**, 34715–34733 (2020).
- 762 54. Pérez, S., Eichhorn, P. & Aga, D. S. Evaluating the biodegradability of sulfamethazine,
763 sulfamethoxazole, sulfathiazole, and trimethoprim at different stages of sewage treatment.
764 *Environ. Toxicol. Chem.* **24**, 1361–1367 (2005).
- 765 55. Lindberg, R. H. *et al.* Behavior of Fluoroquinolones and Trimethoprim during Mechanical,
766 Chemical, and Active Sludge Treatment of Sewage Water and Digestion of Sludge. *Environ.*
767 *Sci. Technol.* **40**, 1042–1048 (2006).
- 768 56. Xu, N. *et al.* Estrogen Concentration Affects its Biodegradation Rate in Activated Sludge.
769 *Environ. Toxicol. Chem.* **28**, 2263–2270 (2009).
- 770 57. Loh, K.-C. & Chua, S.-S. *Ortho* pathway of benzoate degradation in *Pseudomonas putida*:
771 induction of *meta* pathway at high substrate concentrations. *Enzyme Microb. Technol.* **30**, 620–
772 626 (2002).
- 773 58. Banerjee, A. & Ghoshal, A. K. Phenol degradation by *Bacillus cereus*: Pathway and kinetic
774 modeling. *Bioresour. Technol.* **101**, 5501–5507 (2010).
- 775 59. Helbling, D. E., Hammes, F., Egli, T. & Kohler, H.-P. E. Kinetics and Yields of Pesticide
776 Biodegradation at Low Substrate Concentrations and under Conditions Restricting Assimilable
777 Organic Carbon. *Appl. Environ. Microbiol.* **80**, 1306–1313 (2014).

- 778 60. Kundu, K. *et al.* Defining lower limits of biodegradation: atrazine degradation regulated by
779 mass transfer and maintenance demand in *Arthrobacter aurescens* TC1. *ISME J.* **13**, 2236–
780 2251 (2019).
- 781 61. Köck-Schulmeyer, M. *et al.* Occurrence and behavior of pesticides in wastewater treatment
782 plants and their environmental impact. *Sci. Total Environ.* **458–460**, 466–476 (2013).
- 783 62. Desiante, W. L. *et al.* Wastewater microorganisms impact the micropollutant biotransformation
784 potential of natural stream biofilms. *Water Res.* **217**, 118413 (2022).
- 785 63. Toräng, L., Nyholm, N. & Albrechtsen, H.-J. Shifts in Biodegradation Kinetics of the
786 Herbicides MCPP and 2,4-D at Low Concentrations in Aerobic Aquifer Materials. *Environ. Sci.*
787 *Technol.* **37**, 3095–3103 (2003).
- 788 64. Kolvenbach, B. A., Helbling, D. E., Kohler, H.-P. E. & Corvini, P. F.-X. Emerging chemicals
789 and the evolution of biodegradation capacities and pathways in bacteria. *Curr. Opin.*
790 *Biotechnol.* **27**, 8–14 (2014).
- 791 65. Santos, P. M., Blatny, J. M., Di Bartolo, I., Valla, S. & Zennaro, E. Physiological Analysis of
792 the Expression of the Styrene Degradation Gene Cluster in *Pseudomonas fluorescens* ST. *Appl.*
793 *Environ. Microbiol.* **66**, 1305–1310 (2000).
- 794 66. Harb, M., Wei, C.-H., Wang, N., Amy, G. & Hong, P.-Y. Organic micropollutants in aerobic
795 and anaerobic membrane bioreactors: Changes in microbial communities and gene expression.
796 *Bioresour. Technol.* **218**, 882–891 (2016).
- 797 67. Pirete, L. de M. *et al.* Microbial diversity and metabolic inference of diclofenac removal in
798 optimised batch heterotrophic-denitrifying conditions by means of factorial design. *Environ.*
799 *Technol.* **0**, 1–20 (2023).
- 800 68. Kim, D.-W., Thawng, C. N., Lee, K., Wellington, E. M. H. & Cha, C.-J. A novel sulfonamide
801 resistance mechanism by two-component flavin-dependent monooxygenase system in
802 sulfonamide-degrading actinobacteria. *Environ. Int.* **127**, 206–215 (2019).

- 803 69. Sánchez-Osuna, M., Cortés, P., Barbé, J. & Erill, I. Origin of the Mobile Di-Hydro-Pterate
804 Synthase Gene Determining Sulfonamide Resistance in Clinical Isolates. *Front. Microbiol.* **9**,
805 (2019).
- 806 70. Wu, T. *et al.* The sulfonamide-resistance dihydropteroate synthase gene is crucial for efficient
807 biodegradation of sulfamethoxazole by Paenarthrobacter species. *Appl. Microbiol. Biotechnol.*
808 **107**, 5813–5827 (2023).
- 809 71. Huang, Y. *et al.* Strain-level diversity in sulfonamide biodegradation: adaptation of
810 Paenarthrobacter to sulfonamides. *ISME J.* **18**, wrad040 (2024).
- 811 72. Yun, H. *et al.* Functional Characterization of a Novel Amidase Involved in Biotransformation
812 of Triclocarban and its Dehalogenated Congeners in Ochrobactrum sp. TCC-2. *Environ. Sci.*
813 *Technol.* **51**, 291–300 (2017).
- 814 73. Mohanty, S. K. *et al.* Delineation of the Caffeine C-8 Oxidation Pathway in Pseudomonas sp.
815 Strain CBB1 via Characterization of a New Trimethyluric Acid Monooxygenase and Genes
816 Involved in Trimethyluric Acid Metabolism. *J. Bacteriol.* **194**, 3872–3882 (2012).
- 817 74. Chen, C.-C., Dai, L., Ma, L. & Guo, R.-T. Enzymatic degradation of plant biomass and
818 synthetic polymers. *Nat. Rev. Chem.* **4**, 114–126 (2020).
- 819 75. Liang, Y. *et al.* Functional gene diversity of soil microbial communities from five oil-
820 contaminated fields in China. *ISME J.* **5**, 403–413 (2011).
- 821 76. Reis, A. C. *et al.* Comparative genomics reveals a novel genetic organization of the sad cluster
822 in the sulfonamide-degrader ‘Candidatus Leucobacter sulfamidivorax’ strain GP. *BMC*
823 *Genomics* **20**, 885 (2019).
- 824 77. Ghaly, T. M. *et al.* Stratified microbial communities in Australia’s only anchialine cave are
825 taxonomically novel and drive chemotrophic energy production via coupled nitrogen-sulphur
826 cycling. *Microbiome* **11**, 190 (2023).

- 827 78. Sheridan, P. O., Meng, Y., Williams, T. A. & Gubry-Rangin, C. Genomics of soil depth niche
828 partitioning in the Thaumarchaeota family Gagatemarchaeaceae. *Nat. Commun.* **14**, 7305
829 (2023).
- 830 79. Madyastha, K. M. & Sridhar, G. R. A Novel Pathway for the Metabolism of Caffeine by a
831 Mixed Culture Consortium. *Biochem. Biophys. Res. Commun.* **249**, 178–181 (1998).
- 832 80. Aukema, K. G. *et al.* In Silico Identification of Bioremediation Potential: Carbamazepine and
833 Other Recalcitrant Personal Care Products. *Environ. Sci. Technol.* **51**, 880–888 (2017).
- 834 81. Wang, Y., Gao, J., Zhou, S. & Lian, M. Microbial degradation of carbamazepine by a newly
835 isolated of *Gordonia polyophrenivorans*. *Environ. Technol. Innov.* **32**, 103322 (2023).
- 836 82. Bernhardt, R. Cytochromes P450 as versatile biocatalysts. *J. Biotechnol.* **124**, 128–145 (2006).
- 837 83. Stravs, M. A., Pomati, F. & Hollender, J. Biodiversity Drives Micropollutant
838 Biotransformation in Freshwater Phytoplankton Assemblages. *Environ. Sci. Technol.* **53**,
839 4265–4273 (2019).
- 840 84. Wanapaisan, P. *et al.* Synergistic degradation of pyrene by five culturable bacteria in a
841 mangrove sediment-derived bacterial consortium. *J. Hazard. Mater.* **342**, 561–570 (2018).
- 842 85. Yu, K. *et al.* An integrated meta-omics approach reveals substrates involved in synergistic
843 interactions in a bisphenol A (BPA)-degrading microbial community. *Microbiome* **7**, 1–13
844 (2019).
- 845 86. Sun, S. *et al.* Metabolic interactions in a bacterial co-culture accelerate phenanthrene
846 degradation. *J. Hazard. Mater.* **403**, 123825 (2021).
- 847 87. Zhao, C. *et al.* Biological removal of sulfamethoxazole enhanced by *S. oneidensis* MR-1 via
848 promoting NADH generation and electron transfer and consumption. *J. Hazard. Mater.* **426**,
849 127839 (2022).
- 850 88. Liu, X. *et al.* Sulfamethoxazole degradation by *Pseudomonas silesiensis* F6a isolated from
851 bioelectrochemical technology-integrated constructed wetlands. *Ecotoxicol. Environ. Saf.* **240**,
852 113698 (2022).

- 853 89. Murdoch, R. W. & Hay, A. G. Genetic and chemical characterization of ibuprofen degradation
854 by *Sphingomonas Ibu-2*. *Microbiology* **159**, 621–632 (2013).
- 855 90. Stadler, L. B., Delgado Vela, J., Jain, S., Dick, G. J. & Love, N. G. Elucidating the impact of
856 microbial community biodiversity on pharmaceutical biotransformation during wastewater
857 treatment. *Microb. Biotechnol.* **11**, 995–1007 (2018).
- 858 91. Yi, M., Sheng, Q., Lv, Z. & Lu, H. Novel pathway and acetate-facilitated complete atenolol
859 degradation by *Hydrogenophaga* sp. YM1 isolated from activated sludge. *Sci. Total Environ.*
860 **810**, 152218 (2022).
- 861 92. Xu, Y., Radjenovic, J., Yuan, Z. & Ni, B.-J. Biodegradation of atenolol by an enriched
862 nitrifying sludge: Products and pathways. *Chem. Eng. J.* **312**, 351–359 (2017).
- 863 93. Henning, N., Kunkel, U., Wick, A. & Ternes, T. A. Biotransformation of gabapentin in surface
864 water matrices under different redox conditions and the occurrence of one major TP in the
865 aquatic environment. *Water Res.* **137**, 290–300 (2018).
- 866 94. Xu, J.-L. *et al.* *Rhodococcus qingshengii* sp. nov., a carbendazim-degrading bacterium. *Int. J.*
867 *Syst. Evol. Microbiol.* **57**, 2754–2757 (2007).
- 868 95. Wang, Y. *et al.* Toxicity evaluation of the metabolites derived from the degradation of
869 phenanthrene by one of a soil ubiquitous PAHs-degrading strain *Rhodococcus qingshengii* FF.
870 *J. Hazard. Mater.* **415**, 125657 (2021).
- 871 96. Li, G. *et al.* Decolorization and biodegradation of triphenylmethane dyes by a novel
872 *Rhodococcus qingshengii* JB301 isolated from sawdust. *Ann. Microbiol.* **64**, 1575–1586
873 (2014).
- 874 97. Shahabivand, S., Mortazavi, S. S., Mahdavinia, G. R. & Darvishi, F. Phenol biodegradation by
875 immobilized *Rhodococcus qingshengii* isolated from coking effluent on Na-alginate and
876 magnetic chitosan-alginate nanocomposite. *J. Environ. Manage.* **307**, 114586 (2022).
- 877 98. Belovezhets, L. A., Markova, Yu. A., Levchuk, A. A., Oborina, E. N. & Adamovich, S. N. The
878 Effect of Atranes on the Growth of *Rhodococcus qingshengii* VKM Ac-2784D in the Presence

- 879 of Various Carbon Sources and on Its Ability to Degrade Naphthalene. *Microbiology* **91**, 713–
880 720 (2022).
- 881 99. Iminova, L. *et al.* Physiological and biochemical characterization and genome analysis of
882 *Rhodococcus qingshengii* strain 7B capable of crude oil degradation and plant stimulation.
883 *Biotechnol. Rep.* **35**, e00741 (2022).
- 884 100. Kavanagh, K. L., Jörnvall, H., Persson, B. & Oppermann, U. Medium- and short-chain
885 dehydrogenase/reductase gene and protein families. *Cell. Mol. Life Sci.* **65**, 3895 (2008).
- 886 101. Rao, M. R. *et al.* Phytoremediation and phytosensing of chemical contaminants, RDX and
887 TNT: identification of the required target genes. *Funct. Integr. Genomics* **9**, 537–547 (2009).
- 888 102. Kumar, M. *et al.* Genomic and proteomic analysis of lignin degrading and
889 polyhydroxyalkanoate accumulating β -proteobacterium *Pandoraea* sp. ISTKB. *Biotechnol.*
890 *Biofuels* **11**, 154 (2018).
- 891 103. Alhefeiti, M. A., Athamneh, K., Vijayan, R. & Ashraf, S. S. Bioremediation of various
892 aromatic and emerging pollutants by *Bacillus cereus* sp. isolated from petroleum sludge. *Water*
893 *Sci. Technol.* **83**, 1535–1547 (2021).
- 894 104. Ye, H. *et al.* Assessing the biodegradation efficiency and underlying molecular pathway of
895 strain AEPI 0–0: A newly isolated tetracycline-degrading *Serratia marcescens*. *Environ.*
896 *Technol. Innov.* **32**, 103383 (2023).
- 897